SPhT/03-086

Random trees between two walls: Exact partition function

J. Bouttier[1], P. Di Francesco[2] and E. Guitter[3]

Service de Physique Théorique, CEA/DSM/SPhT
Unité de recherche associée au CNRS
CEA/Saclay
91191 Gif sur Yvette Cedex, France

We derive the exact partition function for a discrete model of random trees embedded in a one-dimensional space. These trees have vertices labeled by integers representing their position in the target space, with the SOS constraint that adjacent vertices have labels differing by ± 1. A non-trivial partition function is obtained whenever the target space is bounded by walls. We concentrate on the two cases where the target space is (i) the half-line bounded by a wall at the origin or (ii) a segment bounded by two walls at a finite distance. The general solution has a soliton-like structure involving elliptic functions. We derive the corresponding continuum scaling limit which takes the remarkable form of the Weierstrass $\wp$ function with constrained periods. These results are used to analyze the survival probability of an evolving population spreading in the target spaces (i)-(ii). They also translate, via suitable bijections, into generating functions for bounded planar graphs.

06/03

[1] bouttier@spht.saclay.cea.fr
[2] philippe@spht.saclay.cea.fr
[3] guitter@spht.saclay.cea.fr

1. Introduction

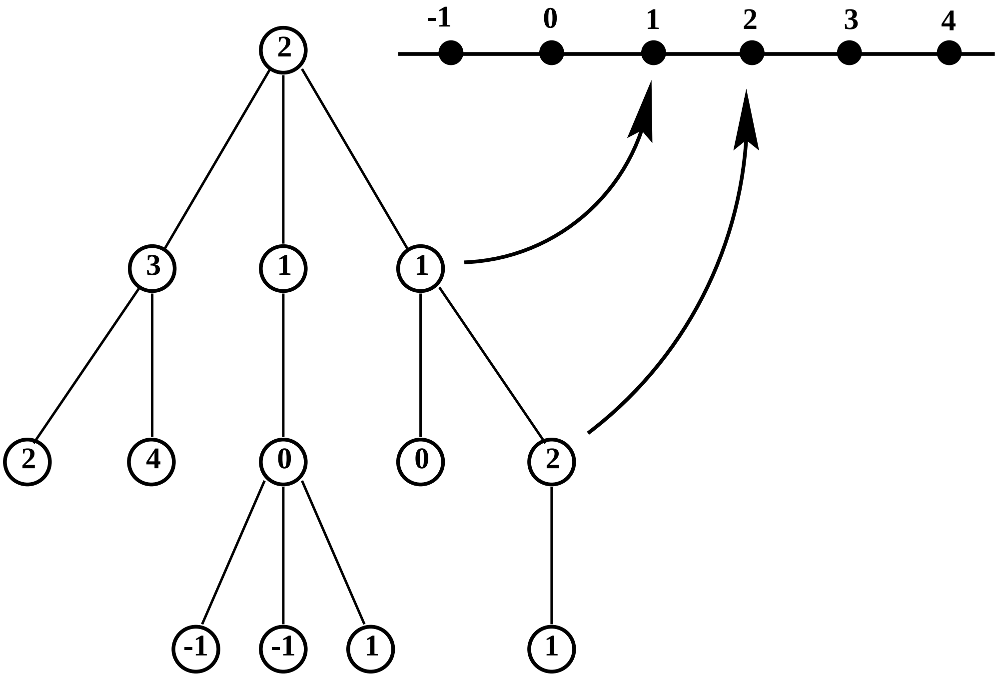

Fig.1: A sample rooted labeled planar tree, with root (top) vertex labeled by 2. Neighboring vertices have labels differing by ± 1. These labels may be viewed as positions on a target integer line as indicated.

In this paper, we consider a simple model describing the embedding in one dimension of a random tree. More precisely, we consider random *rooted* trees whose vertices are labeled by integers representing their possible discrete positions in a one-dimensional target space. We moreover impose that two neighboring vertices on the tree have labels differing by $+1$ or -1, which allows to view the edges of the tree as rigid segments of unit length embedded in the real line (see Fig.1 for an illustration). We choose to consider the case of so-called *planar* trees, i.e. we count as *distinct* all trees obtained by permuting any two descendent subtrees at a given vertex. This model is nothing but a discrete version of the so called one-dimensional Brownian snake [1] which is used to describe branching processes, for instance the spreading of a population in a one-dimensional target space. In this language, we may think of our rooted trees as representing "genealogical trees" for the lineage of an initial individual (materialized by the root vertex), while the labels represent the positions in space of all the descendent individuals. The spreading process is modeled by demanding that each individual lives at distance one from its parent. We will discuss this interpretation in details in section 5 below. Alternatively, we may view this model as an SOS (Solid-On-Solid) model with heights given by the labels, and whose base space is a random tree.

We shall consider a statistical sum over all such trees with a weight g per edge, and with a fixed position, say n, of the root vertex. With no bounds on the labels, the partition function is trivial as it amounts to counting rooted planar trees with N edges (in number c_N where $c_N = \binom{2N}{N}/(N+1)$ is the N-th Catalan number), each of which gives rise to 2^N possible embeddings. The problem becomes more interesting in the presence of a wall, say at position -1, which amounts to imposing that all labels be non-negative. Similar trees were introduced under the name of "well-labeled trees" in Ref.[2] in connection with the enumeration of rooted planar tetravalent graphs, with vertex labels representing the (necessarily non-negative) geodesic distance on the graph to the root vertex[4]. The explicit form of the corresponding partition function as a function of g and n was given in Ref.[3] in the context of planar graph enumeration and will be recalled in the next section. A remarkable outcome of this solution is the emergence of discrete soliton-like expressions, suggesting an underlying integrable structure.

The purpose of this paper is to study the statistics of trees with labels now belonging to a *finite set*, say $\{0, 1, \cdots, L\}$, which amounts to having two walls at positions -1 and $L+1$ in the embedding target space. Such boundary conditions correspond to the so-called RSOS (Restricted Solid-On-Solid) version of the problem, in which heights are restricted to belong to a finite segment.

The paper is organized as follows. In Sect.2, we introduce a master equation for the partition function of labeled rooted trees and recall its solutions both without walls and with one wall. Sect.3 is devoted to the derivation of the two-wall solution, involving elliptic functions. The corresponding continuum limit is derived in Sect.4 and expressed in terms of the Weierstrass $\wp$ function with constrained periods. As an application of these results we study in Sect.5 a particular stochastic process describing the evolution of a population which spreads in one dimension. We gather a few concluding remarks in Sect.6. We first give in Sect.6.1 the solution of a slightly different problem corresponding to a dilute SOS version in which neighboring vertices of the tree have labels differing by ± 1 *or* 0. We then discuss in Sect.6.2 the connection between labeled trees and planar graphs and reinterpret some of our results as partition functions for possibly bounded graphs. Sect.6.3 contains remarks on the integrability of the problem.

---

[4] In this reference, a slightly different constraint is imposed on the labels, demanding that neighboring vertices have labels differing by $0, \pm 1$. Our results will be easily extended to this modified case in the conclusion, with no fundamental difference.

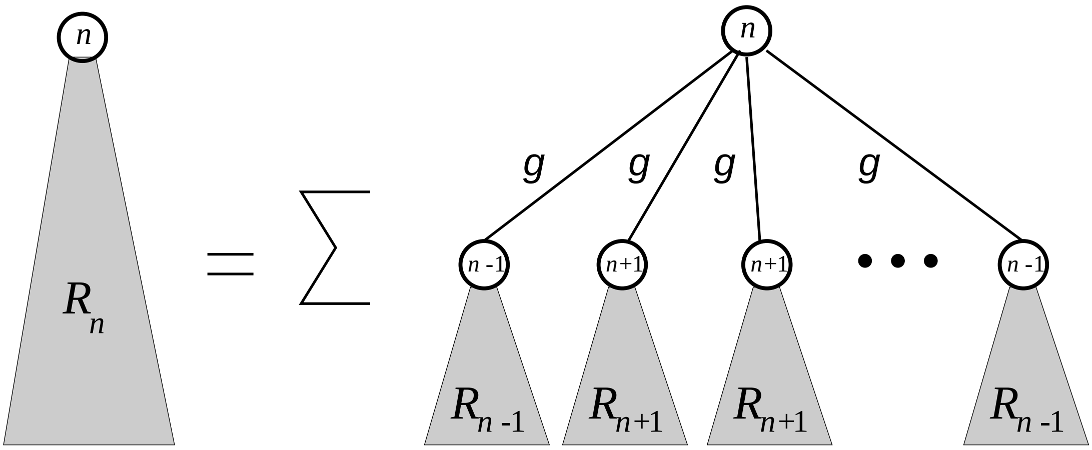

Fig.2: A sketch of the master equation (2.1). A tree contributing to R_n is decomposed according to the sequence of descendents of its root (labeled by n). Each descendent vertex is arbitrarily labeled by $n \pm 1$ henceforth the descendent subtrees are generated by $R_{n\pm1}$ accordingly. Each edge connected to the root is given a weight g. The summation over all possible configurations produces the r.h.s. of eq.(2.1).

2. Enumeration of labeled rooted trees

Let R_n denote the generating function for labeled rooted planar trees with a root at position n. By a decomposition according to the possible local environments of the root vertex, characterized by the sequence of labels $n-1$ or $n+1$ of its adjacent vertices (see Fig.2), we immediately get the equation

$$R_n = \frac{1}{1 - g(R_{n+1} + R_{n-1})} \tag{2.1}$$

Note also that from their combinatorial definition as counting functions, the R_n's are required to have a series expansion in powers of g starting as $R_n = 1 + O(g)$, a condition sufficient to determine all the R_n's from eq.(2.1). The relation (2.1) is valid for all accessible values of n and it may be supplemented by boundary conditions to account for the possible presence of walls. We choose those conditions among three categories: no wall, one wall and two walls, corresponding to restrictions on the allowed labels n, respectively no restriction, $n \geq 0$ and $0 \leq n \leq L$.

In the absence of wall, all the R_n's are equal due to translational invariance, to a function R satisfying $R = 1/(1-2gR)$ and $R = 1 + O(g)$, namely:

$$R = R(g) \equiv \frac{1 - \sqrt{1-8g}}{4g} = \sum_{N=0}^{\infty} g^N 2^N c_N \tag{2.2}$$

This formula displays the critical value $g_c = 1/8$ of g, while the coefficient of g^N clearly counts rooted planar trees with N edges (c_N) with 2^N possible embeddings.

In the presence of one wall at position -1, we must write $R_{-1} = 0$ and consider the equation (2.1) only for $n \geq 0$. This system may be solved order by order in g using as a seed the vanishing of all the coefficients of the series for R_{-1} and the order zero values $R_n = 1 + O(g)$ for all $n \geq 0$. In a more global way, the solution was worked out in Ref.[3] by replacing the condition of existence of a power series expansion for each R_n by the condition that $R_n \to R$ at large n with R as above. Indeed, it is clear from the combinatorial definition that $R - R_n = O(g^{n+1})$ as the wall at position -1 may not be reached with less than $(n+1)$ edges from position n. The solution of eq.(2.1) with these boundary conditions reads:

$$R_n = R \frac{u_n u_{n+4}}{u_{n+1} u_{n+3}}, \quad u_n = x^{\frac{n+1}{2}} - x^{-\frac{n+1}{2}} \tag{2.3}$$

with $R = R(g)$ as in eq.(2.2) and where x is the solution of

$$x + \frac{1}{x} + 2 = \frac{1}{gR} \tag{2.4}$$

with, say, modulus less than 1, namely $x = x(g) \equiv (1 - (1-8g)^{\frac{1}{4}})/(1 + (1-8g)^{\frac{1}{4}})$. Note that x is real for all $g \leq 1/8$ and admits a convergent series expansion in g with *positive integer* coefficients. The small g behavior $x(g) = g + O(g^2)$ ensures the above property that $R_n = R + O(g^{n+1})$. The solution (2.3) is readily checked by noting that eq.(2.1) translates into the following trilinear equation for the u's

$$u_n u_{n+2} u_{n+4} = \frac{1}{R} u_{n+1} u_{n+2} u_{n+3} + gR(u_{n-1} u_{n+3} u_{n+4} + u_n u_{n+1} u_{n+5}) \tag{2.5}$$

easily verified upon substituting $gR = x/(1+x)^2$ and $1/R = (1+x^2)/(1+x)^2$. The particular form of the solution (2.3) was identified in Ref.[3] as a stationary one-soliton solution to the KP equation [4].

In the presence of two walls, we must write $R_{-1} = R_{L+1} = 0$ and consider eq. (2.1) for $0 \leq n \leq L$. This system may again be solved order by order in g from the boundary conditions that all coefficients of R_{-1} and R_{L+1} vanish and $R_n = 1 + O(g)$ for all n, $0 \leq n \leq L$. For a finite value of L, one may also eliminate all but one R_n from the finite set of algebraic equations (2.1) so as to obtain an algebraic equation of degree $[(L+3)/2]$ for each R_n, with a unique solution such that $R_n = 1 + O(g)$. In a more global way, we intend to generalize the solution (2.3) to this two-wall case. This is done in the next section.

3. Two-wall solution

3.1. General solution via elliptic functions

From the one-soliton structure of the solution (2.3), it is natural to look for a more general soliton-like solution to the equation (2.1) in the "elliptic" form

$$
\begin{aligned}
R_n &= R\frac{u_n u_{n+4}}{u_{n+1}u_{n+3}} \\
u_n &= (x^{\frac{n+1}{2}} - x^{-\frac{n+1}{2}})\prod_{j=1}^{\infty}(1-q^j x^{n+1})(1-\frac{q^j}{x^{n+1}})
\end{aligned}
\tag{3.1}
$$

with an additional free real parameter q such that $|q| < 1$. For $q = 0$, we recover the solution (2.3) provided R and x are given by eqns.(2.2) and (2.4), depending on g only. As we shall now see, for a general q, we may tune R and x in eq.(3.1) as functions of *both* g *and* q so as to satisfy the equation (2.1). The above solution clearly satisfies R_{-1}=0 and the value of the free parameter q may finally be adjusted so as to ensure $R_{L+1} = 0$.

To fix the functions R and x in terms of g and q, we again write eq.(2.1) in the form of eq.(2.5), and note that from the definition of u_n, we have $u_{-1} = 0$ and $u_{-2-k} = -u_k$. Hence, taking $n = -1$ in eq.(2.5), we get $gR^2 = u_1/u_3$ while taking $n = -2$, we obtain $gR = (u_0/u_1)^2$, which generalizes eq.(2.4). This leads to:

$$
g = \frac{u_0^4 u_3}{u_1^5}
\tag{3.2}
$$

which implicitly determines $x(g, q)$ as a function of g and q. More precisely, for a fixed q with $0 \leq q < 1$, this equation has four solutions for $0 \leq g \leq 1/8$, a real positive one $x_0(g, q)$ with, say, modulus less than 1 together with its inverse $x_2(g, q) = 1/x_0(g, q)$, and a solution on the unit circle $x_1(g, q)$ with, say, positive imaginary part together with its inverse $x_3(g, q) = 1/x_1(g, q)$. For a fixed q with $-1 < q \leq 0$, we have the same pattern of solutions provided $g \geq 1/8$ and does not exceed some upper bound. When $g = 1/8$, all solutions coalesce to $x = 1$ independently of q. For a definite value of the position L of the second wall, the proper choice of solution will be discussed below. In particular, the presence of two walls at a finite distance increases the radius of convergence of the R_n's as series of g as it reduces the entropy of configurations. This requires exploring values of $g > 1/8$. Note that for $q = 0$, we have $x_0(g, 0) = x(g)$, corresponding to the solution of section 2, while $x_1(g, 0) = (1 + i(1 - 8g)^{\frac{1}{4}})/(1 - i(1 - 8g)^{\frac{1}{4}})$.

The function R is now given by

$$R = \frac{u_1^3}{u_0^2 u_3} \tag{3.3}$$

with two determinations $R^{(0)}(g,q)$ and $R^{(1)}(g,q)$ corresponding respectively to the substitutions $x = x_0(g,q)$ and $x = x_1(g,q)$ in the u_n's, or equivalently $x_2(g,q)$ and $x_3(g,q)$ respectively as the change $x \to 1/x$ amounts to $u_n \to -u_n$, leaving R and all R_n's invariant. It remains to verify that, for these particular choices of x and R, the u_n's of eq.(3.1) actually satisfy the identity (2.5) for all n. Let us introduce the notations $q = e^{2i\pi\tau}$, $x^{n+1} = e^{2i\pi z}$ so that $u_n = \theta_1(z)$ where θ_1 is the (unnormalized) Jacobi theta function with nome q and argument z:

$$\theta_1(z) \equiv \theta(z|\tau) = 2i\sin(\pi z)\prod_{j\geq 1}(1 - 2q^j\cos(2\pi z) + q^{2j}) \tag{3.4}$$

We also introduce the notation $x = e^{2i\pi\alpha}$, so that eq.(2.5), together with the particular choices (3.2) and (3.3), translates into a theta function identity

$$\begin{aligned}\left(\frac{\theta_1(2\alpha)}{\theta_1(\alpha)}\right)^2 \theta_1(z)\theta_1(z+2\alpha)\theta_1(z+4\alpha) = \frac{\theta_1(4\alpha)}{\theta_1(2\alpha)}\theta_1(z+\alpha)\theta_1(z+2\alpha)\theta_1(z+3\alpha)\\ + \theta_1(z-\alpha)\theta_1(z+3\alpha)\theta_1(z+4\alpha) + \theta_1(z)\theta_1(z+\alpha)\theta_1(z+5\alpha)\end{aligned} \tag{3.5}$$

To prove it, we note that both hands have the same transformations when $z \to z+1$ and $z \to z+\tau$, due to the properties $\theta_1(z+1) = -\theta_1(z)$ and $\theta_1(z+\tau) = -q^{-\frac{1}{2}}e^{-2i\pi z}\theta_1(z)$. Taking the ratio of rhs/lhs of eq.(3.5), we get an elliptic function, with poles possibly at $z = 0, -2\alpha, -4\alpha$ in a fundamental cell. One easily checks by examining the rhs at these values that the corresponding residues all vanish and therefore the ratio is a constant, easily shown to be 1 by taking for instance its value at $z = -\alpha$, which completes the proof of the identity. With these notations, we have the relations

$$g = \frac{\theta_1^4(\alpha)\theta_1(4\alpha)}{\theta_1^5(2\alpha)} \tag{3.6}$$

and

$$R = \frac{\theta_1(2\alpha)^3}{\theta_1(\alpha)^2\theta_1(4\alpha)} \tag{3.7}$$

while

$$R_n = \frac{\theta_1(2\alpha)^3}{\theta_1(\alpha)^2\theta_1(4\alpha)}\,\frac{\theta_1((n+1)\alpha)\theta_1((n+5)\alpha)}{\theta_1((n+2)\alpha)\theta_1((n+4)\alpha)} \tag{3.8}$$

with $\theta_1(z)$ as in eq.(3.4). As this solution involves elliptic functions, it is natural to study its transformation under the modular transformation $\tau \to -1/\tau$. From the transformation $\theta_1(z/\tau|-1/\tau) = -i(-i\tau)^{1/2} e^{i\pi z^2/\tau}\theta_1(z|\tau)$, we find that the *physical quantities* such as g as given by eq.(3.6) above and R_n as given by eq.(3.8) are invariant under $(\alpha,\tau) \to (\tilde{\alpha},\tilde{\tau}) \equiv (\alpha/\tau, -1/\tau)$ or equivalently $(x,q) \to (\tilde{x},\tilde{q})$ with $\tilde{x} = x^{1/\tau}$ and $\tilde{q} = e^{-2i\pi/\tau}$. This is not the case for intermediate factors such as R or any of the u_n's taken independently. We deduce from these properties that the *same* solution is reached by the parameters (x,q) and by their modular transforms $(\tilde{x},\tilde{q})$.

It is interesting to study the modular transformation of the solutions $x_i(g,q)$, $i = 0,1,2,3$ of eq.(3.6) as introduced above. Clearly, for a fixed g, the modular invariance of the r.h.s. of eq.(3.6) implies that $\tilde{x}_i(g,q) = x_i(g,q)^{1/\tau}$ is a valid solution when $q \to \tilde{q}$, hence we may write $x_i(g,q)^{1/\tau} = x_{\sigma(i)}(g,\tilde{q})$ for some permutation $\sigma \in S_4$. Iterating this transformation, and using $\tilde{\tilde{q}} = q$ while $\tau\tilde{\tau} = -1$, we deduce that $x_{\sigma^2(i)}(g,q) = x_i(g,q)^{-1}$, which brings us back to the same solution we started from, but with the determination $x_i(g,q)^{-1}$ instead of $x_i(g,q)$. Therefore σ is a *circular permutation* of the four indices.

For $q < 0$, the modular transform $\tilde{q}$ becomes complex, and we will make no use of the above remarks. On the other hand, for $0 < q < 1$, the modular parameter $\tau = it$ may be taken purely imaginary, and the modular transformation reduces to $t \to 1/t$ hence $\tilde{q}$ is also real and in the range $(0,1)$. It is then easy to see that the modular transformation sends the solution $x_0(g,q)$ to $x_1(g,\tilde{q})$ and $x_1(g,q)$ to $x_2(g,\tilde{q})$ which leads to the same R_n's as $x_0(g,\tilde{q})$. In other words, the same physical solution may be described by either some q and the real determination $x_0(g,q)$ or by its modular transform $\tilde{q}$ and the determination on the unit circle $x_1(g,\tilde{q})$.

3.2. Boundary condition at $n = L+1$

We now implement the two-wall boundary condition described above, in which we require $R_{L+1} = 0$, or equivalently $u_{L+5} = 0$. This is achieved by demanding that $x^{L+6} = q^m$ for some $m \in \mathbb{Z}$. From the above study, we have at our disposal x-solutions either real positive and smaller than 1, or on the unit circle with positive imaginary part (we discard the equivalent $1/x$-solution). This leaves us for *positive* q with two possibilities: (i) $x = e^{2i\pi\frac{k}{L+6}}$, $k = 1,2,...$ corresponding to $m = 0$ and (ii) $x = q^{\frac{m}{L+6}}$, $m = 1,2,...$ while at *negative* q, only the solution (i) survives. As the solution R_n must be positive by definition for $n = 0,1,...,L$, it is easily verified that only $k = 1$ in case (i) and $m = 1$ in case (ii) are admissible to prevent sign changes for the u_n's and the R_n's. In a more physical language, higher values of k or m correspond to higher modes with oscillations in the range $[0,L]$. Taking for instance $m=2$ corresponds to a first vanishing of R_n at the coordinate $n=L/2-2$.

For any given L, we may always pick the solution (i) and define $q_L(g)$ as the unique real solution of

$$x_1(g,q_L(g))=e^{\frac{2i\pi}{L+6}} \tag{3.9}$$

Introducing the notation $L(g)$ for the value of L such that $x_1(g,q=0)=e^{\frac{2i\pi}{L+6}}$, namely

$$L(g)=\frac{\pi}{\arctan\left((1-8g)^{\frac{1}{4}}\right)}-6 \tag{3.10}$$

we have that $q_L(g)>0$ for $L>L(g)$ and $q_L(g)<0$ for $L<L(g)$, also valid for $g>1/8$ with the convention that $L(g)=\infty$ in this range. The length $L(g)$ may be taken as a measure of the typical extent in the embedding space of the random trees at a fixed value of g, in the absence of walls.

On physical grounds, we expect a qualitative change of behavior to occur at wall distances L of the order of $L(g)$. For $L>>L(g)$, the tree behaves as a compact object of typical extent $L(g)$ "diffusing" between the walls and feeling them only when approaching at distances of the order of $L(g)$ and smaller. For $L<<L(g)$, the walls strongly squeeze the tree and L is the only relevant scale of the problem. In the first regime, the *profile* $\{R_n\}_{0\leq n\leq L}$, always maximal in the middle, is mainly constant and decreased significantly only at distances of order $L(g)$ from the walls. In the second regime, the profile will vary over the whole range between the walls. Alternatively, for a fixed value of L, we may invert these conditions into $q_L(g)>0$ for $g<g_L$ and $q_L(g)<0$ for $g>g_L$, where

$$g_L=\frac{1}{8}\left(1-\tan^4\left(\frac{\pi}{L+6}\right)\right) \tag{3.11}$$

Note that $0<g_L<1/8$ for all $L=0,1,2,...$

Beside the solution (3.9) above, we have another possibility for the choice of q namely $q=q'_L(g)$ which solves the condition (ii)

$$x_0(g,q'_L(g))=q'_L(g)^{\frac{1}{L+6}} \tag{3.12}$$

This alternative solution exists for all $L>L(g)$ and is a priori distinct from the previous solution (3.9). In practice, the *physical solution* for fixed g and L is *unique* as one easily checks that the solution (3.9) is the modular transform of (3.12), namely $q_L(g) = \tilde{q'}_L(g)$ and $x_1(g, q_L(g)) = x_0(g, q'_L(g))^{\frac{1}{\tau'_L(g)}}$ with $q'_L(g) = e^{2i\pi\tau'_L(g)}$. The two choices (3.9) or (3.12) therefore lead to the same physical quantities R_n.

To obtain the combinatorial series expansions for the R_n's in g it is simpler to work with the solution (3.12). This is always possible as g is small (hence we may work in the regime $g < g_L$). Moreover, we have $x_0(g, q'_L(g)) = g + O(g^2)$ while $q'_L(g) = g^{L+6}(1+O(g))$. This shows in particular that the present R_n and the former $R(g)$ of eq.(2.2) have the same expansion up to order $\mathrm{Min}(n+1, L-n+1)$ in g, as expected.

On the other hand, to have a more global approach it is best to work with the solution (3.9), which is valid for any g. We may then use the relations (3.6)-(3.8) with $\alpha = 1/(L+6)$ to parametrize the solution with q as follows

$$
\begin{aligned}
g(q) &= \frac{\theta_1^4\left(\frac{1}{L+6}\right)\theta_1\left(\frac{4}{L+6}\right)}{\theta_1^5\left(\frac{2}{L+6}\right)} \\
R(q) &= \frac{\theta_1^3\left(\frac{2}{L+6}\right)}{\theta_1^2\left(\frac{1}{L+6}\right)\theta_1\left(\frac{4}{L+6}\right)} \\
R_n(q) &= \frac{\theta_1^3\left(\frac{2}{L+6}\right)}{\theta_1^2\left(\frac{1}{L+6}\right)\theta_1\left(\frac{4}{L+6}\right)} \frac{\theta_1\left(\frac{n+1}{L+6}\right)\theta_1\left(\frac{n+5}{L+6}\right)}{\theta_1\left(\frac{n+2}{L+6}\right)\theta_1\left(\frac{n+4}{L+6}\right)}
\end{aligned}
\tag{3.13}
$$

with θ_1 as in eq.(3.4). This form displays clearly the symmetry $R_n = R_{L-n}$ expected from the symmetry of the problem, as a consequence of the relation $\theta_1(1-z) = \theta_1(z)$.

For fixed L, the function $g(q)$ starts from $g = 0$ at $q = 1$ and increases as q decreases, passing through g_L of eq.(3.11) at $q = 0$, and reaching a maximum value $g_c(L) > 1/8$ attained at some negative value of $q = q_c(L)$ (see Fig.3 for illustration). The quantity $g_c(L)$ is nothing but the radius of convergence of all the series in g appearing in the problem, and governs the leading growth of the number of configurations as a function of the number N of edges in the tree as $g_c(L)^{-N}$. We have for instance $g_c(1) = 1/4$, $g_c(2) = 3 - 2\sqrt{2}$, $g_c(3) = 4/27$. We also see that $g_c(L) \to 1/8$ when $L \to \infty$. The branch of the solution for $q < q_c(L)$ is discarded as unphysical.

To conclude this section, let us use the solution (3.13) to display for fixed L the exact profile $\{R_n\}_{0 \le n \le L}$ for some particular values of q, namely

(a) a positive value of q realizing $g < g_L$, in which case the profile is flat except for a region distant by typically $L(g)$ from the walls

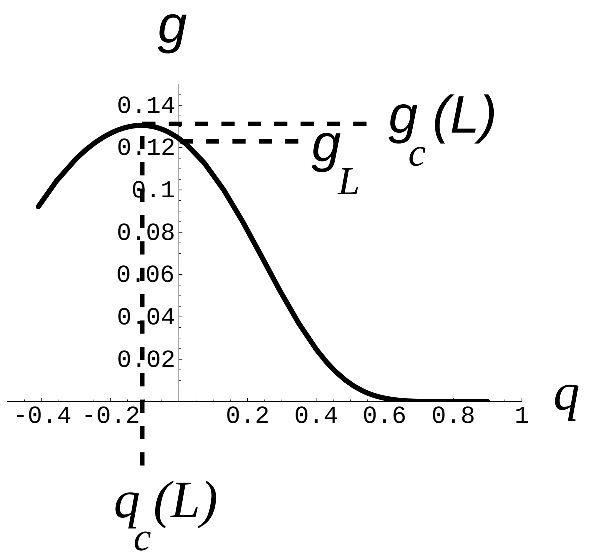

Fig.3: Plot of $g(q)$ as given by eq.(3.13) for $L = 6$. The function decreases from a maximum value $g_c(L)$ at some negative value $q_c(L)$ down to 0 at $q = 1$. At $q = 0$, we have $g = g_L$ as in eq.(3.11). We have $g_L < \frac{1}{8} < g_c(L)$.

(b) the value $q = 0$ where $g = g_L$ and all theta functions degenerate into trigonometric functions

(c) the negative value $q = q_c(L)$ corresponding to $g = g_c(L)$, where the profile varies over the whole range $[0, L]$ and is slightly peaked in the middle

These profiles are represented in Fig.4 for $L = 100$.

4. Continuum limit

For starters, let us derive the continuum limit of the one-wall solution (2.3). It is reached by letting $g \to 1/8$ and $n \to \infty$ simultaneously as:

$$g = \frac{1}{8}(1 - \epsilon^4), \qquad n = \frac{r}{\epsilon} \tag{4.1}$$

with $\epsilon \to 0$ playing the role of the inverse of a correlation length. This leads to

$$x(g) = \frac{1 - \epsilon}{1 + \epsilon}, \qquad R(g) = \frac{2}{1 + \epsilon^2} \tag{4.2}$$

and finally, expanding R_n up to order 2 in ϵ:

$$R_n = 2(1 - \epsilon^2 \mathcal{U}(r)) \tag{4.3}$$

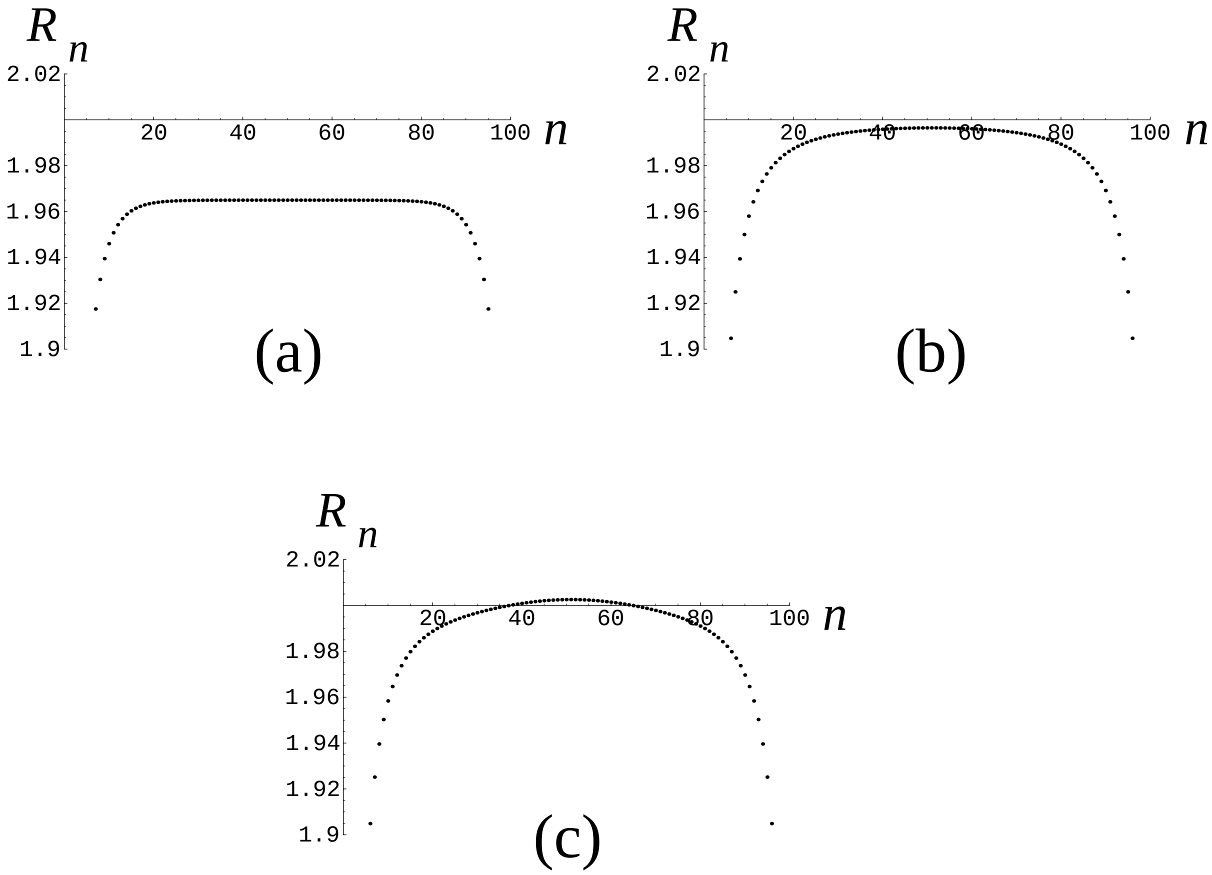

Fig.4: Typical profiles $\{R_n\}_{0\leq n\leq L}$ for $L=100$ as obtained from eq.(3.13) for three particular values of q: (a) a positive value realizing $g\leq g_L$ where the profile is flat except for a region of extent $L(g)$ from the walls (here $q=.25$ and $L(g)\simeq 18$) (b) $q=0$ ($g=g_L$) and (c) $q=q_c(L)$ ($g=g_c(L)$) where the profile is slightly peaked in the middle.

where $\mathcal{U}$ is the scaling function

$$\mathcal{U}(r)=1+\frac{3}{\sinh^2(r)} \tag{4.4}$$

describing the "repulsive potential" felt by the tree as a function of the rescaled distance r from the wall at $r=0$.

In the presence of the second wall, we let in addition $L\to\infty$ by keeping the quantity $\omega=(L+6)\epsilon/2$ fixed. This ratio of the two characteristic lengths of the problem, namely L and the typical extent of the unconstrained tree $L(g)\sim\pi/\epsilon$ is the only physical scale surviving the continuum limit. Expanding the rhs of the first line of equation (3.13) at small ϵ up to order 4, we get

$$g = \frac{1}{8}\left(1 - \frac{\epsilon^4}{\omega^4}\left(\frac{5}{32}\left(\frac{\theta_1'''(0)}{\theta_1'(0)}\right)^2 - \frac{3}{32}\frac{\theta_1^{(5)}(0)}{\theta_1'(0)}\right)\right) \tag{4.5}$$

to be identified with $g = 1/8(1-\epsilon^4)$ as in eq.(4.1). This fixes implicitly the value of τ as a function of ω by

$$\omega^4 = \frac{5}{32}\left(\frac{\theta_1'''(0)}{\theta_1'(0)}\right)^2 - \frac{3}{32}\frac{\theta_1^{(5)}(0)}{\theta_1'(0)} \tag{4.6}$$

We may now expand R and R_n as given by eq.(3.13) up to order 2 in ϵ to obtain the relevant scaling function

$$\begin{aligned} R &= 2\left(1 - \frac{\epsilon^2}{4\omega^2}\frac{\theta_1'''(0)}{\theta_1'(0)}\right) \\ R_n &= 2\left(1 - \epsilon^2 \mathcal{U}(r)\right) \end{aligned} \tag{4.7}$$

with r as in eq.(4.1) and where the scaling function $\mathcal{U}(r)$ is now given by

$$\mathcal{U}(r) = \frac{\theta_1'''(0)}{4\omega^2\theta_1'(0)} - 3\frac{d^2}{dr^2}\mathrm{Log}\,\theta_1\left(\frac{r}{2\omega}\right) = 3\wp(r) \tag{4.8}$$

where we have identified the Weierstrass $\wp$ function [5] with half-periods ω and $\omega' = \tau\omega$ where τ is fixed by eq.(4.6), which amounts to

$$g_2(\omega, \omega') = \frac{4}{3} \tag{4.9}$$

where g_2 is the first elliptic invariant of the Weierstrass function. The scaling function $\mathcal{U}(r)$ may be viewed as the potential felt by the random tree in the presence of the two walls.

When sending the second wall to infinity, i.e. taking $\omega \to \infty$, we immediately recover the above result (4.4) as $g_2 = 4/3$ fixes the second half-period $\omega' = i\pi/2$, in which case the scaling function degenerates into (4.4). Taking $L = L(g)$, i.e. $\omega = \pi/2$, fixes $\omega' = i\infty$ which corresponds to $q = 0$, in which case the scaling function degenerates into a trigonometric function

$$\mathcal{U}(r) = \frac{3}{\sin^2(r)} - 1 \tag{4.10}$$

The values of $\omega \in [\pi/2, \infty]$ ($L \geq L(g)$) correspond to taking $q \in [0,1]$, while those in $[0, \pi/2]$ ($L \leq L(g)$) are obtained for $q \in [-q_*, 0]$, where $q_* = \lim_{L\to\infty} q_c(L) = e^{-\pi\sqrt{3}}$.

Note that we could have derived the scaling limit of R_n without using the explicit solution (3.13) by plugging the ansatz $R_n = 2(1 - \epsilon^2 \mathcal{U}(r))$ in the original equation (2.1) and expanding up to order 4 in ϵ to obtain a differential equation for $\mathcal{U}$, namely

$$\mathcal{U}'' = 2(\mathcal{U}^2 - 1) \tag{4.11}$$

and require that $\mathcal{U}(r)$ diverge at $r = 0$ and $r = 2\omega$, with no divergence in-between. This equation is to be compared with that satisfied by $\wp$, namely $\wp'' = 6\wp^2 - g_2/2$, which allows to identify $\mathcal{U}(r) = 3\wp(r)$ provided $g_2 = 4/3$.

5. A simple application: survival probability in a spreading population

As mentioned in the introduction, labeled rooted planar trees may be used to model a branching evolution process in which an initial parent individual (materialized by the root vertex) gives rise in one generation to a number $k \geq 0$ of children individuals with probability p_k, each child itself independently giving rise to subsequent generations with the same probabilities. The resulting genealogical tree is nothing but a *planar* tree (without labels). In the following, we concentrate on the particular case $p_k = (1-p)p^k$, with $0 \leq p \leq 1$, and where the prefactor $(1-p)$ ensures the correct normalization and may be interpreted as the probability of death without descendents.

Moreover, we let the individuals sit on the integer line, with the diffusion rule that each child lives at a position differing by ± 1 from that of its parent, with an equal probability 1/2. Using these positions as vertex labels, we may write the following master equation for the extinction probability of a family

$$E_n(T) = \frac{1-p}{1 - \frac{p}{2}(E_{n+1}(T-1) + E_{n-1}(T-1))} \tag{5.1}$$

where $E_n(T)$ stands for the probability that an individual sitting at position n has no more descendent at generation T, with the initial condition $E_n(0) = 0$. Eq.(5.1) is obtained by enumerating all possible configurations of the first generation children, and noting that the joint probability of extinction of all their descendents is the product of individual extinction probabilities before generation $T-1$. Comparing eq.(5.1) to eq.(2.1), we see that $E_n \equiv \lim_{T\to\infty} E_n(T)$ obeys the same equation (2.1) as $(1-p)R_n$, provided we set

$$g = \frac{p(1-p)}{2} \tag{5.2}$$

This allows to identify $E_n = (1-p)R_n$ by noting that this choice corresponds precisely to the stable fixed point of the recursion relation (5.1). We may therefore interpret $(1-p)R_n$ as the probability of extinction of a family whose first generation's parent sits at position n. Accordingly, we interpret $S_n = 1-(1-p)R_n$ as the survival probability for such a family.

For unconstrained positions (no wall in the former language), we simply have a translation invariant probability of survival

$$S_n = S(p) \equiv \frac{2p-1+|2p-1|}{2p} = \begin{cases} 0 & p \in [0, \frac{1}{2}] \\ \frac{2p-1}{p} & p \in [\frac{1}{2}, 1] \end{cases} \tag{5.3}$$

obtained by substituting $g = p(1-p)/2$ into eq.(2.2). This result is totally insensitive to the diffusion process, and is the same as that for unlabeled trees. It displays a first order singularity (discontinuous derivative) at $p = p_c = \frac{1}{2}$. This classical result in the theory of branching processes [6] is a particular case of a more general statement for so-called Galton-Watson processes that the genealogical tree is almost surely finite (here $S(p) = 0$) if and only if the average number of children is less or equal to one (here corresponding to $\sum jp_j = p/(1-p) \leq 1$, namely $p \leq 1/2$).

The introduction of wall-type boundary conditions is a natural way to create a non-trivial coupling of the survival rate to the diffusion process. One possibility is that when a child reaches the position of a wall it becomes immortal, and thus ensures the survival of its whole family forever. Putting a wall at position say $n = -1$, the above condition is achieved by imposing that the extinction probability $E_{-1}(T)$ be 0 independently of T. Another interpretation consists in viewing the family as a population of pathogenic bacteria spreading from a germ at position n, while an initially healthy organism sits at position -1. The probability for the organism to remain uninfected after T generations of bacteria is readily seen to obey eq.(5.1) with boundary condition $E_{-1}(T) = 0$, but has a different initial value at $T = 0$, namely $E_n(0) = 1$ for $n \geq 0$. We expect however no difference for the $T \to \infty$ limit of the solution. The survival probability of the family $S_n = 1 - E_n(T = \infty)$ may therefore also be interpreted as the probability of infection of the organism. The wall boundary condition $E_{-1} = 0$ precisely corresponds to our former choice to take $R_{-1} = 0$. The solution (2.3) leads to the family's survival probability (or alternatively to the healthy organism's probability of getting infected)

$$S_n = 1 - \frac{1-|2p-1|}{2p} \frac{(1-x^{n+1})(1-x^{n+5})}{(1-x^{n+2})(1-x^{n+4})} \tag{5.4}$$

where

$$x = x(p) \equiv \frac{1 - |2p-1|^{\frac{1}{2}}}{1 + |2p-1|^{\frac{1}{2}}} \tag{5.5}$$

Note that for any fixed $n \geq 0$ the survival probability S_n is strictly positive as soon as $p > 0$, and moreover that it still displays a singularity at $p = p_c = 1/2$ but of weaker *third order* type (discontinuity of the third derivative) as is readily seen by expanding S_n up to order 3 in powers of $|2p-1|$. Note also the following simple expression for the survival probability at the transition point $p = \frac{1}{2}$:

$$S_n(p = \frac{1}{2}) = \frac{3}{(n+2)(n+4)}, \quad n \geq 0 \tag{5.6}$$

The scaling limit (4.1) may be used to study the vicinity of the transition point by setting $p = p_c(1 + \eta\epsilon^2)$ with $\eta = \pm 1$ according to whether we approach the transition from above or below. Eq.(4.3) allows to interpret the scaling function $\mathcal{U}(r)$ as describing the scaling behavior of the survival probability $S_n \sim \mathcal{S}_n$ around $p = \frac{1}{2}$, with

$$\mathcal{S}_n = \epsilon^2(\mathcal{U}(n\epsilon) + \eta) = |2p-1| \left(\frac{3}{\sinh^2(n|2p-1|^{1/2})} + 1 \right) + (2p-1) \tag{5.7}$$

valid in the scaling region of large n and $n\epsilon = O(1)$. This scaling function displays clearly the above-mentioned third order transition with

$$\mathcal{S}_n = \frac{3}{n^2} + (2p-1) + \frac{n^2}{5}(2p-1)^2 - \frac{2n^4}{63}|2p-1|^3 + O((2p-1)^4 n^6) \tag{5.8}$$

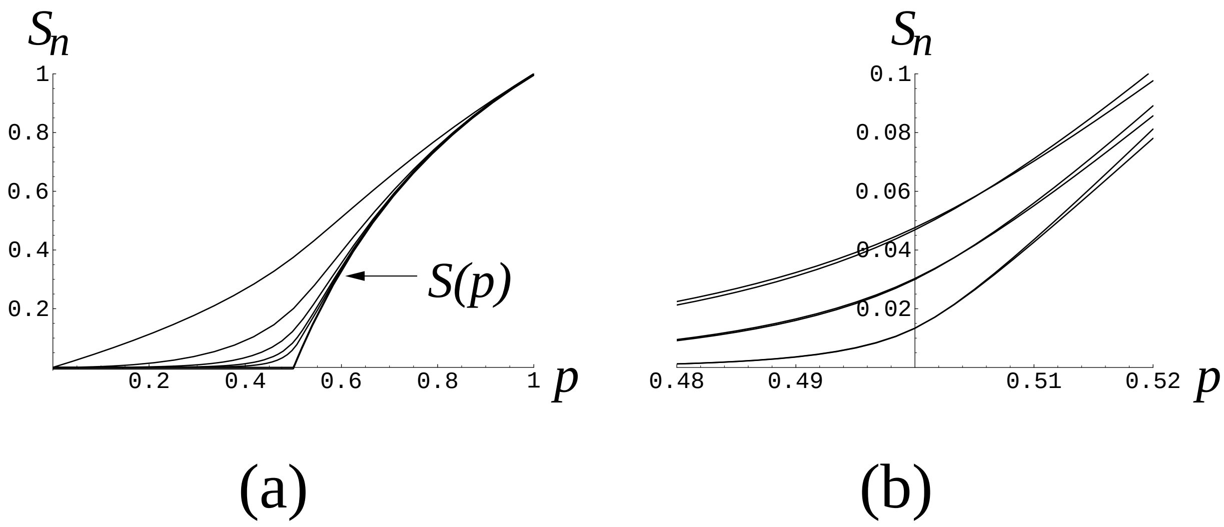

Fig.5: Survival probabilities S_n of eq.(5.4) as functions of p in the presence of one wall, (a) for $p \in [0,1]$ and from top to bottom $n = 0,1,2,3,4$ as well as $n = \infty$ in which case we recover the no-wall solution $S(p)$ of eq.(5.3); (b) for p in the critical region $p \sim \frac{1}{2}$ and from top to bottom $n = 5,7,12$, together with the expected scaling limits $\mathcal{S}_n$ as given by eq.(5.7) with a proper shift of $n \to n+3$ ensuring the perfect matching of the curves.

We have represented in Fig.5 the survival probabilities $S(p)$ and $S_n(p)$ as functions of $p \in [0,1]$, respectively in the cases without and with a wall. We have also blown out the critical region around $p = 1/2$ to compare the exact solution with its scaling limit.

In the presence of two immortalizing walls at positions -1 and $L+1$, the solution (3.13) leads directly to the survival probability $S_n = 1-(1-p)R_n$. This is also the probability for *at least one* of two healthy organisms sitting at positions -1 and $L+1$ to get infected by a family of bacteria spreading from an initial germ at position n.

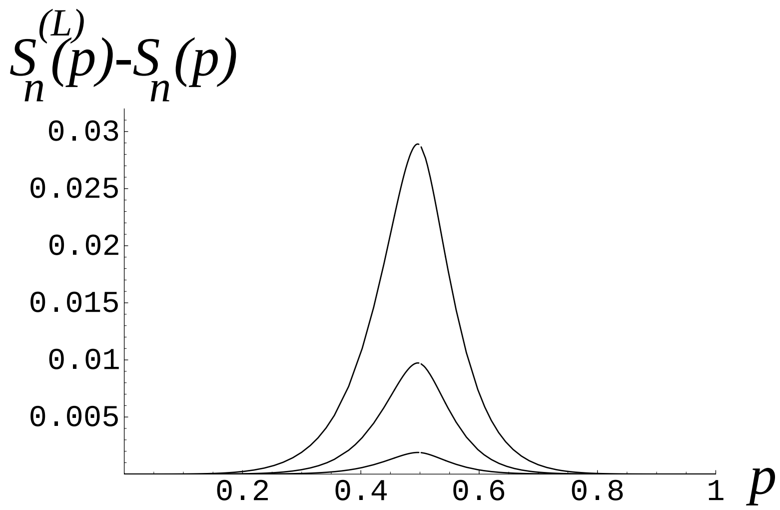

Fig.6: Plot of the increase in the probability of survival $S_n^{(L)}(p) - S_n(p)$ from the one-wall situation to that with two walls for $L = 5$ and $n = 0, 1, 2$ (bottom to top).

For illustration, we have displayed in Fig.6 the increase in the probability of survival $S_n^{(L)}(p) - S_n(p)$ from the one-wall situation to that with two walls for $L = 5$ and $n = 0, 1, 2$, as functions of $p \in [0,1]$. The increase is maximal at $p = \frac{1}{2}$.

For finite L, the critical value $g_c(L) > 1/8$ is never attained as $g = p(1-p)/2 \in [0, 1/8]$ for $p \in [0,1]$, hence the singularity at $p = \frac{1}{2}$ is suppressed. However it is restored in the scaling limit where $L \to \infty$ with $L|2p-1|^{1/2}$ fixed, as $g_c(L) \to 1/8$ in this case. The scaling function $\mathcal{U}(r)$ given by eq.(4.8) again describes the scaling behavior of the survival probability in the vicinity of $p = \frac{1}{2}$, with the result:

$$\mathcal{S}_n = 3|2p-1|\wp(n|2p-1|^{1/2}) + (2p-1) \tag{5.9}$$

where the Weierstrass $\wp$ function must be taken with fixed half-periods $\omega = L|2p-1|^{1/2}/2$ and $\omega' = \tau\omega$, such that $g_2(\omega,\omega') = \frac{4}{3}$. We again note that $\mathcal{S}_n$ displays a third order singularity at $p = \frac{1}{2}$ by expanding

$$\mathcal{S}_n = \frac{3}{n^2} + (2p-1) + \frac{3}{20} g_2(\omega,\omega') n^2 (2p-1)^2 + \frac{3}{28} g_3(\omega,\omega') n^4 |2p-1|^3 + O((2p-1)^4 n^6) \quad (5.10)$$

where g_2 and g_3 stand for the elliptic invariants of the Weierstrass function and with the constraint that $g_2(\omega,\omega') = 4/3$ which fixes ω' and consequently g_3 as functions of $\omega = L|2p-1|^{1/2}/2$. Note that the singularity of $\mathcal{S}_n$ at $p = 1/2$ disappears at the modular invariant point $\tau = i$ i.e. $q = e^{-2\pi}$, where $g_3(\omega, i\omega) = 0$, which causes all odd powers of $|2p-1|$ to vanish in the series expansion (5.10).

Of particular simplicity is the case when $q = 0$ in eq.(3.13), corresponding to $g = g_L$ as in eq.(3.11), i.e. $p = (1 - \tan^2(\pi/(L+6)))/2$ or $p = (1 + \tan^2(\pi/(L+6)))/2$. The formula for the associated survival probability reads

$$\mathcal{S}_n = \begin{cases} \frac{1}{\cos\left(\frac{2\pi}{L+6}\right)} \left(\frac{\sin\left(\frac{\pi}{L+6}\right)\sin\left(\frac{3\pi}{L+6}\right)}{\sin\left(\pi\frac{n+2}{L+6}\right)\sin\left(\pi\frac{n+4}{L+6}\right)} - 2\sin^2\left(\frac{\pi}{L+6}\right)\right) & p = \frac{1}{2}\left(1 - \tan^2\left(\frac{\pi}{L+6}\right)\right) \\ \frac{\sin\left(\frac{\pi}{L+6}\right)\sin\left(\frac{3\pi}{L+6}\right)}{\sin\left(\pi\frac{n+2}{L+6}\right)\sin\left(\pi\frac{n+4}{L+6}\right)} & p = \frac{1}{2}\left(1 + \tan^2\left(\frac{\pi}{L+6}\right)\right) \end{cases} \quad (5.11)$$

This allows for framing the exact value of S_n at $p = 1/2$ between these two values for all L. For large L, we may identify $\omega = \lim_{L\to\infty} L|2p-1|^{1/2}/2 = \pi/2$ for both values of $p = (1 \pm \tan^2(\pi/(L+6)))/2$, and $\tau = i\infty$ to ensure $q = 0$, in which case the scaling function reduces to (4.10) and therefore eq.(5.9) turns into

$$\mathcal{S}_n = |2p-1| \left(\frac{3}{\sin^2(n|2p-1|^{1/2})} - 1 \right) + (2p-1) \quad (5.12)$$

in agreement with the large L limit of eq.(5.11).

6. Conclusion

6.1. Another solvable case of tree embedding

We may consider a slightly different version of the problem in which we impose the weaker constraint that any two adjacent vertices of the tree must have labels differing by ± 1 *or* 0. In the language of spreading of a population, a child may now stay at the same position as its parent. This corresponds to a sort of dilute SOS version of the case studied in this paper. The main recursion relation is now replaced by

$$R_n = \frac{1}{1 - g(R_{n+1} + R_n + R_{n-1})} \tag{6.1}$$

where R_n is the generating function for rooted trees with root vertex labeled by $n \in \mathbb{Z}$, and a weight g per edge. Again, we may consider three types of boundaries: no wall, one wall and two walls. The no-wall case is easily solved, with all the R_n's equal to the solution of $R = 1/(1 - 3gR)$ with $R = 1 + O(g)$, namely

$$R = R(g) \equiv \frac{1 - \sqrt{1 - 12g}}{6g} \tag{6.2}$$

The one-wall case corresponds to setting $R_{-1} = 0$ and only considering the R_n's for $n \geq 0$. It was solved in Ref.[3], with the result

$$R_n = R\frac{u_n u_{n+3}}{u_{n+1}u_{n+2}}, \qquad u_n = x^{\frac{n+1}{2}} - x^{-\frac{n+1}{2}} \tag{6.3}$$

with $R = R(g)$ of eq.(6.2), and where x is the solution of $x + 1/x + 4 = 1/(gR)$ with, say, modulus less than 1. Note the slight difference in the index shifts when compared with eq. (2.3). The main recursion relation reduces this time to a quartic equation for the u_n's:

$$u_n u_{n+1} u_{n+2} u_{n+3} = \frac{1}{R} u_{n+1}^2 u_{n+2}^2 + gR(u_{n-1}u_{n+2}^2 u_{n+3} + u_n^2 u_{n+3}^2 + u_n u_{n+1}^2 u_{n+4}) \tag{6.4}$$

supplemented by the initial condition $u_{-1} = 0$. Eq.(6.4) is easily checked for all k by setting $1/R = (x^2 + x + 1)/(x^2 + 4x + 1)$ and $gR = x/(x^2 + 4x + 1)$. Finally, in the two-wall case where we require $R_{-1} = R_{L+1} = 0$ and only consider $n = 0, 1, 2, ..., L$, we have found the elliptic solution

$$\begin{aligned} R_n &= R\frac{u_n u_{n+3}}{u_{n+1}u_{n+2}} \\ u_n &= \theta_1((n+1)\alpha) \end{aligned} \tag{6.5}$$

with $x = e^{2i\pi\alpha}$ and θ_1 as in eq.(3.4), and which solves eq.(6.4) provided we take

$$\begin{aligned} R &= 4\frac{\theta_1(\alpha)\theta_1(2\alpha)}{\theta_1'(0)\theta_1(3\alpha)}\left(\frac{\theta_1'(\alpha)}{\theta_1(\alpha)} - \frac{1}{2}\frac{\theta_1'(2\alpha)}{\theta_1(2\alpha)}\right) \\ g &= \frac{\theta_1'(0)^2\theta_1(3\alpha)}{16\theta_1(\alpha)^2\theta_1(2\alpha)\left(\frac{\theta_1'(\alpha)}{\theta_1(\alpha)} - \frac{1}{2}\frac{\theta_1'(2\alpha)}{\theta_1(2\alpha)}\right)^2} \end{aligned} \tag{6.6}$$

The boundary conditions are again satisfied for two choices of the parameter x: (i) $x = e^{2i\pi/(L+5)}$ and (ii) $x = q^{1/(L+5)}$ (when $q \geq 0$), the latter leading to the same physical solution as the former by modular invariance. Picking again the first solution, we must take $\alpha = 1/(L+5)$, and may view the equations for the solution as parametrized by q. This leads to the continuum limit, upon taking $g = (1-\epsilon^4)/12$, $n = r/\epsilon$, $2\omega = (L+5)\epsilon$ and $R_n = 2(1-\epsilon^2\mathcal{U}(r))$. We end up with a scaling function $\mathcal{U}(r) = 2\wp(r)$ in terms of the Weierstrass $\wp$ function with half-periods ω as above and ω' fixed by now requiring that $g_2(\omega,\omega') = 3$. We also recover the one-wall case by taking the limit $L \to \infty$, namely $\omega = \infty$ while $\omega' = i\pi/\sqrt{6}$, in which case $\mathcal{U}(r) = 1 + 3/\sinh^2(\sqrt{3/2}r)$, a result already obtained in Ref.[3].

6.2. Graph interpretation

As mentioned in the introduction, well-labeled trees, i.e. trees with non-negative labels corresponding to the one-wall situation in the dilute SOS version of Sect.6.1 were introduced in Ref.[2] in the context of graph enumeration. More precisely, it was shown that there exists a bijection between these well-labeled rooted planar trees and rooted planar quadrangulations. This allows to interpret the quantity R_n of eq.(6.3) as the generating function for planar quadrangulations with both a marked (origin) vertex and a marked oriented edge linking a vertex with geodesic distance m from the origin to a vertex with geodesic distance $m+1$ from the origin with $m \leq n$, and with an activity g per vertex. Beside this equivalence, there exists yet another bijection, now in the dual language, between rooted planar tetravalent graphs (dual to the above quadrangulations) and decorated (so-called blossom-) binary trees [7]. This bijection was extended so as to keep track of geodesic distances between faces in Ref.[3]. In this language, the generating function Z_n for two-leg planar tetravalent graphs with the two legs distant by at most n was shown to obey the recursion relation $Z_n = 1 + gZ_n(Z_{n+1} + Z_n + Z_{n-1})$, with $Z_{-1} = 0$, a direct consequence of the above bijection with blossom binary trees. This equation is nothing but yet another form of eq.(6.1) and allows to identify $Z_n = R_n$ of eq.(6.3).

Remarkably, our slightly simpler equation (2.1) also admits two analogous interpretations in terms of graphs, now related to the enumeration of rooted planar Eulerian triangulations (i.e. triangulations with bi-colored faces, say in black and white) or dually to that of rooted trivalent bipartite planar graphs (say with black and white vertices). In this dual language, we may rely on a bijection [8] between rooted trivalent bipartite planar graphs and properly decorated binary trees. Keeping track of the graph-geodesic distances in these binary trees leads to the equation $Z_n = 1 + gZ_n(Z_{n+1} + Z_{n-1})$ for the generating function Z_n of two-leg trivalent bi-colored planar graphs with the two legs attached to vertices of opposite colors and at geodesic distance at most n. In this approach, the proper definition of the geodesic distance on the graphs makes use of oriented paths linking faces, with the constraint that a step across an edge between two faces always leaves the black vertex on the left. The equation for Z_n is yet another form of eq.(2.1) which allows to identify $Z_n = R_n$ of eq.(2.3).

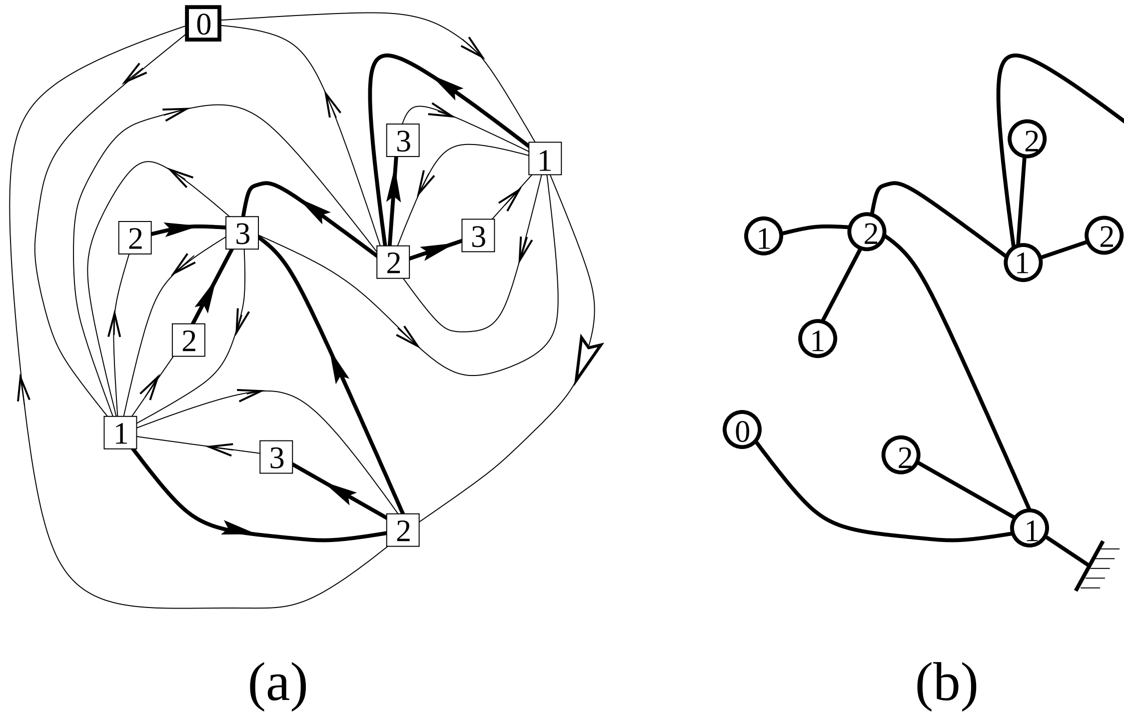

Fig.7: A sample Eulerian triangulation (a) with a marked origin vertex (labeled 0) and a marked oriented edge (big empty arrow). We have indicated for each vertex its geodesic distance from the origin (respecting the edge-orientations). A labeled rooted tree (b) is obtained by retaining for each clockwise-oriented triangle the edge connecting the two farthest vertices from the origin, and picking as the root the end of the previously marked edge. The vertex labels on the tree are simply the distances of the graph vertices from the origin minus one.

In terms of triangulations, a bijection similar to that of Ref.[2] may be established between rooted planar Eulerian triangulations and the well-labeled (SOS) trees corresponding to the one-wall situation of Sect.2 as follows. First we replace the face-bicoloration by the compatible orientation of all edges in such a way that each triangle is either clockwise- or counterclockwise oriented. This allows to define the geodesic distance from a vertex to another as the length of a minimal path respecting the orientation of edges. Picking as origin some vertex, a well-labeled tree is obtained by retaining for each clockwise-oriented triangle the edge linking the two farthest vertices from the origin, and labeling each vertex by its distance from the origin minus one, as illustrated in Fig.7 (see Ref.[9] for details and proofs). This allows to interpret R_n as the generating function for planar Eulerian triangulations with a marked (origin) vertex and a marked oriented edge linking a vertex with geodesic distance m from the origin to a vertex with geodesic distance $m+1$ from the origin with $m \leq n$, and with an activity g per vertex.

In the language of graphs, we may use our two-wall solutions to enumerate *bounded* graphs as follows. The quantity

$$G_n^{(L)} = R_n^{(L)} - R_{n-1}^{(L-1)} \tag{6.7}$$

where $R_n^{(L)}$ is the solution of eq.(2.1) (resp. (6.1)) with two walls at positions -1 and $L+1$, is the generating function for Eulerian triangulations (resp. for quadrangulations) with a marked (origin) vertex, a marked oriented edge linking a vertex with geodesic distance n from the origin to a vertex with geodesic distance $n+1$ from the origin and which are "bounded" in the sense that the geodesic distance of *all the vertices* from the origin is less or equal to $L+1$. As an example, the rooted Eulerian triangulation of Fig.7 contributes to $G_1^{(L)}$ for all $L \geq 2$.

6.3. Integrability and matrix models

The striking simplicity of the solutions (2.3)(3.1) as well as (6.3)(6.5) are directly linked to the "integrability" of the corresponding non-linear recursion relations (2.1) and (6.1) respectively. As already discussed in Ref.[3] in the context of graph enumeration, these equations are very similar to those arising in the context of matrix models, namely $R_n = (n/N)/(1-g(R_{n+1}+R_{n-1}))$, where N is the size of the matrices. The remarkable point is that the index n is no longer related to the geodesic distance along the graphs as in Sect.6.2, but to their *genus*. Soliton theory seems to indicate that integrability survives when changing the recursion into $R_n = (\alpha+\beta n)/(1-g(R_{n+1}+R_{n-1}))$ for some constants α and β, which could interpolate between the two problems.

Beyond the two (quadratic) examples of this paper, we have at our disposal a host of non-linear recursion relations all used for enumerating possibly decorated planar graphs while keeping track of some geodesic distances, and which were found to be integrable as well (see Ref.[3] for details). The solutions display some multicritical behavior corresponding to higher order critical points, with non-trivial hierarchies of scaling functions. It would be interesting to find some proper interpretation of those equations in the context of embedded tree-like objects or alternatively of population-spreading processes.

References

[1] See e.g. J.-F. Le Gall,*Spatial Branching Processes, Random Snakes and Partial Differential Equations*, Birkhauser, Boston (1999).

[2] P. Chassaing and G. Schaeffer, *Random Planar Lattices and Integrated SuperBrownian Excursion*, preprint (2002), to appear in Probability Theory and Related Fields, math.CO/0205226.

[3] J. Bouttier, P. Di Francesco and E. Guitter, *Geodesic distance in planar graphs*, to appear in Nucl. Phys. B, cond-mat/0303272.

[4] See e.g. M. Jimbo and T. Miwa, *Solitons and infinite dimensional Lie algebras*, Publ. RIMS, Kyoto Univ. **19** No. 3 (1983) 943-1001, eq.(2.12).

[5] H. Bateman, *Higher Transcendental Functions*, vol. II, McGraw-Hill, New-York (1953).

[6] S. Karlin and H. Taylor, *A first course in stochastic processes*, Academic Press, New-York (1975).

[7] G. Schaeffer, *Bijective census and random generation of Eulerian planar maps*, Electronic Journal of Combinatorics, vol. **4** (1997) R20; see also G. Schaeffer, *Conjugaison d'arbres et cartes combinatoires aléatoires* PhD Thesis, Université Bordeaux I (1998).

[8] M. Bousquet-Mélou and G. Schaeffer, *Enumeration of planar constellations*, Adv. in Applied Math., **24** (2000) 337-368; see also D. Poulalhon and G. Schaeffer, *A note on bipartite Eulerian planar maps*, preprint (2002), *http://www.loria.fr/~schaeffe/* and J. Bouttier, P. Di Francesco and E. Guitter, *Counting colored Random Triangulations*, Nucl.Phys. **B641** (2002) 519-532.

[9] J. Bouttier, P. Di Francesco and E. Guitter, in preparation.